Characterization of an *Escherichia coli* Sulfite Oxidase Homologue Reveals the Role of a Conserved Active Site Cysteine in Assembly and Function†

Stephen J. Brokx, Richard A. Rothery, Guijin Zhang, Derek P. Ng, and Joel H. Weiner*

Membrane Protein Research Group, Department of Biochemistry, 474 Medical Sciences Building, University of Alberta, Edmonton, Alberta, T6G 2H7, Canada

Received April 4, 2005; Revised Manuscript Received May 26, 2005

ABSTRACT: We report the biochemical and biophysical characterization of YedYZ, a sulfite oxidase homologue from *Escherichia coli*. YedY is a soluble catalytic subunit with a twin arginine leader sequence for export to the periplasm by the Tat translocation system. YedY is the only molybdoenzyme so far isolated from *E. coli* with the Mo-MPT form of the molybdenum cofactor. The electron paramagnetic resonance (EPR) signal of the YedY molybdenum is similar to that of known Mo-MPT containing enzymes, with the exception that only the Mo(IV) → Mo(V) transition is observed, with a midpoint potential of 132 mV. YedZ is a membrane-intrinsic cytochrome *b* with six putative transmembrane helices. The single heme *b* of YedZ has a midpoint potential of −8 mV, determined by EPR spectroscopy of YedZ-enriched membrane preparations. YedY does not associate strongly with YedZ on the cytoplasmic membrane. However, mutation of the YedY active site Cys102 to Ser results in very efficient targeting of YedY to YedZ in the membrane, demonstrating a clear role for YedZ as the membrane anchor for YedY. Together, YedYZ comprise a well-conserved bacterial heme-molybdoenzyme found in a variety of bacteria that can be assigned to the sulfite oxidase class of enzyme.

The facultative anaerobe *Escherichia coli* is capable of anaerobic respiratory growth using terminal electron acceptors such as fumarate, nitrate, and dimethyl sulfoxide (DMSO).[1] The terminal reductases required for growth on these acceptors are fumarate reductase (FrdABCD) (*1*−*3*), nitrate reductase (NarGHI) (*4*), and DMSO reductase (DmsABC) (*5*), respectively. These enzymes are membrane-associated multisubunit oxidoreductases with several redox active cofactors including heme, flavins, iron−sulfur clusters, and molybdo-bis(molybdopterin guanine dinucleotide) (Mo-bisMGD).

Molybdenum-containing oxidoreductases are found throughout nature, and in all cases, with the exception of nitrogenase, the molybdenum atom is coordinated in the protein by molybdopterin (MPT) (*6*, *7*), which is typically found in its tricyclic pyranopterin form (*8*, *9*). Eukaryotic molybdoenzymes provide molybdenum atom coordination via the two dithiolene sulfurs of a single MPT. Additional coordination can be provided by a protein−molybdenum ligand, such as a Cys residue, and by oxo, hydroxyl, and sulfido groups. In prokaryotes, most molybdoenzymes studied to date provide coordination via four dithiolene sulfurs from a total of two MPT moieties. This bis-MPT coordination is complicated by the covalent addition of a nucleotide (guanine or cytidine) to each MPT moiety via a phosphodiester bond. Additional molybdenum ligands are provided by amino acid side chains (Ser, Cys, or Asp) and oxo and hydroxyl groups (*8*−*10*).

The determination of the *E. coli* genome sequence (*11*) led to the recognition of a large number of genes of unknown function. We have examined the *E. coli* genome for potential novel molybdoenzymes. One unknown open reading frame identified in this search was *yedY* (Blattner number b1971), which is part of the putative *yedYZ* operon. The genes for this operon were cloned from *E. coli* HB101 chromosomal DNA, and the YedY and YedZ proteins were investigated. We have recently reported the purification and structural determination of YedY (*12*). YedY is the soluble periplasmic catalytic subunit of the oxidoreductase and contains a Mo-MPT cofactor, and as such, it is the first Mo-MPT enzyme isolated from *E. coli*. YedY is a member of the sulfite oxidase class of molybdoenzyme (*9*), which is able to catalyze the reduction of S- and *N*-oxides (*12*). In this study, we further examine the biochemical and biophysical characteristics of YedY and describe the characterization of the heme-containing intrinsic membrane subunit YedZ. Together, these two proteins form a well-conserved bacterial oxidoreductase.

† This work was funded by the Canadian Institutes of Health Research and the Institute of General Medical Sciences of the National Institutes of Health. J.H.W. is a Canada Research Chair in Membrane Biochemistry.

* Corresponding author: J. H. Weiner, Department of Biochemistry, University of Alberta, Edmonton, Alberta, T6G 2H7, Canada. Phone, +1-780-492-2761; fax, +1-780-492-0886; e-mail, joel.weiner@ualberta.ca.

[1] Abbreviations: DMSO, dimethyl sulfoxide; EPR, electron paramagnetic resonance; HALS, highly anisotropic low spin; HOQNO, 2-*n*-heptyl-4-hydroxyquinoline *N*-oxide; IPTG, isopropyl-*β*-D-thiogalactoside; MGD, molybdopterin-guanine dinucleotide; MOPS, 3-(*N*-morpholino)propanesulfonic acid; MPT, molybdopterin; ORF, open reading frame; PCR, polymerase chain reaction; PMSF, phenylmethylsulfonyl fluoride; SDS−PAGE, sodium dodecyl sulfate polyacrylamide gel electrophoresis; TMAO, trimethylamine-*N*-oxide.

10.1021/bi050621a CCC: $30.25
Published on Web 07/07/2005

Table 1: List of *E. coli* Strains

E. coli strain	genotype	reference
MG1655	*F*$^-$ λ^- *ilvG rfb50 rph1*	laboratory collection
HB101	*supE44 hsdS20* (r_B^- m_B^-) *recA13 ara-14 proA2 lacY1 galK2 rpsL20 xyl-5 mtl-1 thr-1 leuB6* Δ(*proA2*) *sbcC201 tsx-33 sbcB15*	laboratory collection
TG1	Δ(lac-pro) *supE thi hsd15*/*F′ traD36proAB lacI*^{q} *lacZ* DM15	laboratory collection
DSS640	as TG1; Δ*tatABCD* (Δ*mttA1A2BC*)::*cat*	*16*
MC4100	F$^-$ *araD139* Δ(*argF-lac*)*U169 rpsL150 relA1 ftB3501 deoC1 ptsF25 rbsR*	laboratory collection
TP1000	as MC4100; Δ*mobAB*::*kan* (Kn^R)	*38*
SJB12	as MC4100; Δ*yedYZ*::*cat* (Cm^R)	this study
SJB20	as TG1; Δ*mobAB*::*kan* (Kn^R)	this study

Table 2: List of Oligonucleotide Primers[a]

primer name	sequence
DN3	TATCGTATG*CGATCG*GTGGAAGCGTG
SB1	CGGCTCTTGCTGGCTAACGACAAAAAAGTGT GATGGCTTGTGTAGGCTGGAGCTGCTTC
SB2	CCGGCAGGGATAACGCGTACTTTGTCGGCAA TATGAAGCATATGAATATCCTCCTTAG
SB3	CG*GGATCC*AGGAGAG*GATATC*ATGAAAAAGA ATCAATTT
SB4	CTC*CTCGAG*TACAGATAATTTGTTG
SB5	CGC*CTCGAG*CAAATTCTCCCGCAA
SB6	CGC*GGATCC*GTGTGATGG*CATATG*AAAAAG
SB7	CGCGCCACATC*CTGCAG*GGATAAC
SB8	GTATCGTGGCCT*AGATCT*GCGGGAGAA
SB9	TTCTCCCGC*AGATCT*AGGCCACGATAC

[a] In all cases, the restriction sites found in the oligonucleotides are in script font.

EXPERIMENTAL PROCEDURES

Materials. Molecular biology reagents including restriction endonucleases, T4 DNA ligase, and *Taq* DNA polymerase were purchased from Invitrogen. *Pfu* DNA polymerase was purchased from Stratagene. Anti-pentaHis antibody was supplied by Qiagen, and Western immunoblot horseradish peroxidase reagents were supplied by Pierce. Oligonucleotides were obtained from the DNA Core Facility, Department of Biochemistry, University of Alberta, Canada. All other reagents were of the highest purity commercially available.

Methods. Preparation of bacterial growth media, molecular biology procedures (plasmid DNA isolation, restriction enzyme digestions, polymerase chain reaction, etc.), sodium dodecyl sulfate polyacrylamide gel electrophoresis (SDS−PAGE), and Western immunoblotting were performed by standard procedures (*13*). Protein concentrations were determined by a modification of the Lowry method (*14*).

List of Strains. The *E. coli* bacterial strains used in this study are shown in Table 1.

Cloning of yedYZ Operon. The *yedYZ* genes were cloned into plasmids in different combinations using the oligonucleotide primers shown in Table 2.

The *yedYZ* operon was amplified from *E. coli* HB101 genomic DNA by polymerase chain reaction (PCR), using the oligonucleotides SB3 and SB4. The amplified DNA fragment was cleaved with *Bam*HI and *Xho*I and ligated into a modified pMS119EH plasmid (*15*), which contained a previously engineered hexahistidine tag sequence (*16*). The resulting plasmid, pMSYZH6, contained *yedY* and *yedZ* with expression controlled by the *ptac* promoter of pMS119. YedZ also contains the extra amino acid residues LEHHHHHH after the C-terminal Val residue. Histidine-tagged *yedY* was also cloned without *yedZ* into pMS119 using the primers SB3 and SB5 to yield the plasmid pMSYH6. The *yedYZ* genes were amplified by PCR from HB101 DNA using the primers SB6 and SB7 and cloned into the *Nde*I and *Pst*I restriction sites of the expression plasmid pT7-7, to obtain plasmid pYEDT7 with the untagged *yedYZ* genes controlled by the T7 promoter. The small *Sph*I/*Pst*I fragment of pYEDT7, containing the a 3′ portion of *yedY* and a 5′ portion of *yedZ*, was "swapped" by ligation with the analogous fragment of pMSYZH6 to obtain pMSYZ, which contained the native *yedYZ* genes under the control of the *ptac* promoter of pMS119.

A *Bgl*II restriction site was constructed within the *yedY* gene near the 3′ end in the plasmid pMSYZ, using the primers SB8 and SB9, by the QuikChange site-directed mutagenesis method (Stratagene, La Jolla, CA). The resulting plasmid obtained was pMSYZB. The smaller *Nco*I/*Bgl*II fragment, containing a 3′ portion of *yedY*, was excised from pMSYZB and replaced with the similar *Nco*I/*Bgl*II fragment from pMSYH6 to create the pMSYZ3 plasmid, containing a His_6-tagged YedY and a native YedZ in the pMS119 vector.

Site-Directed Mutagenesis of YedY. The *Sst*I/*Xho*I fragment of pMSYZ3, containing *yedY* was subcloned into pT7Blue-3 (Novagen) to create plasmid pYED5 for mutagenesis and sequencing. The Cys102Ser mutant of YedY was constructed with the primers DN3 and M13 Reverse in the plasmid pYED5 using the QuikChange site-directed mutagenesis method, except that the two primers were not complementary. The mutated DNA fragment, confirmed by sequencing, was then replaced back into pMSYZ3 to create pMSYZ3(C102S).

Creation of Mutant E. coli Strains. A stable *yedYZ* deletion of *E. coli* MC4100, SJB12, was constructed by replacing the operon with the chloramphenicol resistance (CAT) cartridge, by the protocol of Datsenko and Wanner (*17*), using the oligonucleotides SB1 and SB2 as primers. The deletion was confirmed by PCR.

The *mobA*$^-$ *E. coli* strain TP1000 was a kind gift from Dr. Tracey Palmer. The Δ*mobA*::*kan* gene fragment was transferred from TP1000 to *E. coli* TG1 by P1 transduction (*18*) to create the strain SJB20. The *mobA*$^-$ phenotype was confirmed by the ability of this strain to grow anaerobically on glycerol fumarate medium (*19*) but not on glycerol−nitrate medium, because nitrate reductase requires the *mobA* gene product for MGD biosynthesis (*20*).

Amplified Expression and Purification of YedY and YedZ. HB101 or SJB20 cells, transformed with the pMSYZ3 plasmid, were grown in Terrific Broth (*13*) with the addition of 0.003% (w/v) metal ions mixture (*19*), except the ammonium molybdate was replaced with 1 mM Na_2MoO_4. They were grown in 2 L media in 6 L flasks, with shaking at 200 rpm, at 30 °C until $OD_{600} \sim 0.8$. Then isopropyl-β-D-thiogalactoside (IPTG) was added to 0.1 mM, and the cells were incubated for a further 12 h before harvesting. The cell pellet was washed in 100 mM MOPS and 5 mM EDTA, pH 7.0, and a periplasmic fraction, containing soluble, processed $YedYHis_6$, was obtained by the cold osmotic shock procedure (*13*). Briefly, the cells were suspended in 30 mM

Tris, pH 7.5, 1 mM EDTA, 0.2 mM phenylmethylsulfonyl fluoride (PMSF), and 20% (w/v) sucrose and incubated at room temperature with gentle shaking for 10 min. The cells were pelleted by centrifugation, resuspended in ice-cold 1 mM $MgSO_4$, and incubated on ice with gentle shaking for 15 min. The suspension was centrifuged, and the supernatant represented the periplasmic fraction. To the periplasmic fraction, MOPS buffer, pH 7.0, was added to 20 mM, and NaCl was added to 0.5 M. This solution was applied to a column containing 20 mL Chelating Sepharose resin (Amersham-Pharmacia). The column was washed with 20 mM MOPS, 0.5 M NaCl, and 5 mM histidine (pH 7.0), and YedYHis_6 was eluted with the same buffer containing 40 mM histidine.

The cells (with or without periplasm) were resuspended in 100 mM MOPS, 5 mM EDTA, and 0.2 mM PMSF and ruptured by passage through a French Pressure cell at 12 000 psi. Supernatants and membranes were prepared by ultracentrifugation at 150 000*g* as previously described (*21*). Membrane pellets, containing amplified YedZ, were dark red. The membrane fraction was homogenized in the same buffer without PMSF and layered on top of a 55% (w/v) sucrose cushion as described (*22*). After ultracentrifugation for 1.5 h at 150 000*g*, the floating band containing enriched cytoplasmic membrane was isolated, diluted in buffer, and subjected to two further rounds of ultracentrifugation at 150 000*g* for 1.5 h to ensure complete removal of the sucrose.

Spectroscopy. Ultralow temperature (10−50 K) EPR spectra of *E. coli* membranes enriched in YedZ, as well as the Mo(V) spectrum presented in Figure 4, were recorded using a Bruker Elexys E500 spectrometer equipped with an Oxford Instruments ESR-900 flowing helium cryostat. EPR spectra of potentiometrically poised YedY were recorded using a Bruker ESP300E spectrometer equipped with a Bruker liquid nitrogen evaporating cryostat (Bruker ER4111 VT Variable Temperature Unit). Redox titrations were carried out as previously described (*22*). UV−visible spectroscopy was performed using a Hewlett-Packard 8453 diode array spectrophotometer.

Kinetic Analysis. Substrate-dependent oxidation of reduced benzyl viologen ($BVH^{\bullet +}$) was analyzed by an open cuvette assay essentially as described (*23*, *24*). Oxidized benzyl viologen (0.2 mM) was reduced with the addition of sodium dithionite (0.33 mM) in degassed 50 mM MOPS buffer, pH7.0. Substrate-dependent oxidation of $BVH^{\bullet +}$ ($\epsilon_{570\ nm} = 7.8 \times 10^3$ L mol^{-1} cm^{-1}) was monitored using a Jenway 6300 spectrophotometer.

RESULTS

Bioinformatic Analysis of yedYZ. The *yedY* gene was originally identified in a bioinformatics screen of the *E. coli* genome for potential molybdenum-containing proteins. *yedY* and *yedZ* (b1971 and b1972, respectively) form a putative operon starting at 43.9 min (2037.5 kb) of the *E. coli* genome (*11*), with the *yedZ* ORF overlapping the *yedY* ORF by one nucleotide. *yedY* encodes a 334 amino acid pre-protein with a molecular weight of 37.4 kDa. YedY has a putative twin arginine signal peptide for processing by the Tat/Mtt protein translocation apparatus (*25*, *26*). The twin arginine motif has a sequence of KRRQVLK, which agrees with the consensus sequence of (S/T)RR*X*FLK (*27*). The predicted cleavage site is AAHA↓DLL, resulting in a mature protein of 290 amino acid residues and a molecular weight of 32.5 kDa, which was confirmed by electrospray mass spectrometry and N-terminal sequencing (*12*).

In this study, *yedY* was cloned from *E. coli* HB101, a hybrid of K and B strains. We noted a discrepancy from the published *E. coli* K12 MG1655 sequence of *yedY* (*11*), namely, a cytosine to adenosine substitution at position 1205, resulting in a YedY protein with Asp in place of Ala at residue 319 of the unprocessed protein. In other *E. coli* strains, YedY from K12 W3110 (*28*) has Ala at that residue, but in the pathogenic strains O157:H7 (*29*, *30*) and CFT073 (*31*), the residue is an Asp. It appears that the residue at this position may be quite variable and not well-conserved, but commonly a hydrophilic residue. A recent BLASTP search (*32*) of the GenBank database showed that YedY has homologues (≥40% identical) of unknown function in more than 40 bacterial genomes, mostly proteobacteria.

As revealed by the BLAST search, the proteins of known function to which YedY is most homologous are sulfite oxidases from the bacterium *Starkeya novella* (*33*) and higher eukaryotes, including the chicken liver enzyme (*10*, *34*) and assimilatory nitrate reductases, such as that from spinach (*35*). Identity of YedY to these oxidoreductases is approximately 20% over a span of about 170 amino acids. This region encodes the domain responsible for binding a molybdenum-molybdopterin (Mo-MPT) cofactor found in the structure of sulfite oxidases from chicken mitochondria (*10*) and *Arabidopsis thaliana* peroxisomes (*36*) determined by X-ray crystallography. As shown by the YedY crystal structure (*12*), Cys146 or Cys102 in the mature protein provides a sulfur ligand for the molybdenum atom of the Mo-MPT cofactor in a manner analogous to active site cysteines of the sulfite oxidases.

Like YedY, homologues of YedZ of unknown function are found in many bacterial species, as part of an analogous *yedYZ* operon. The conservation in YedZ, approximately 30%, is less than that of YedY. YedZ is a 24.1 kDa protein with six transmembrane helices as predicted by the program TmPred (http://www.ch.embnet.org/software/TMPRED_form.html), with the N- and C-termini predicted to face the cytoplasm (Figure 1). This topology has also been confirmed by PhoA and GFP fusion protein analysis (*37*). YedZ has a theoretical isoelectric point (pI) of 10.8, with several conserved histidine and arginine residues, features which are characteristic of an integral membrane cytochrome. There are three histidine residues which are conserved in YedZ and its bacterial orthologs, histidines 91, 151, and 164 of YedZ. It is very likely that His91 in transmembrane segment 3 and either His151 or His164, both of which are predicted to be in transmembrane segment 5, serve as histidine ligands for a heme moiety. The presence of a heme subunit is not surprising; the *S. novella* sulfite oxidase has a soluble *c*-type cytochrome (SorB) as part of the SorAB enzyme, while other sulfite oxidases and assimilatory nitrate reductases have a heme *b* domain in the single subunit oxidoreductase. In all cases, direct electron transfer between the heme and the molybdenum cofactor is observed.

Cloning and Expression of yedYZ. The *yedYZ* genes were cloned from *E. coli* HB101 chromosomal DNA as described in the Experimental Procedures. Plasmid pMSYZ3, with a histidine-tagged YedY and a native YedZ in the IPTG-

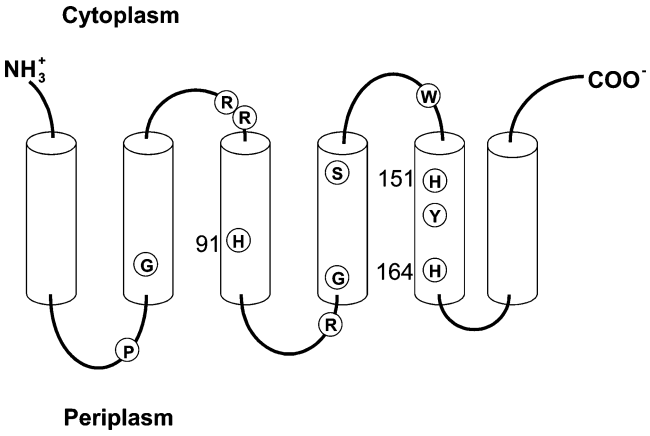

FIGURE 1: Membrane topology of YedZ. Topology was predicted using the program TmPred (http://www.ch.embnet.org/software/TMPRED_form.html), and the tubes represent putative transmembrane helices. Circled letters indicate amino acid residues which are conserved in a ClustalW alignment of YedZ and homologues from other bacteria. Conserved histidine residues, which may coordinate a heme, are numbered.

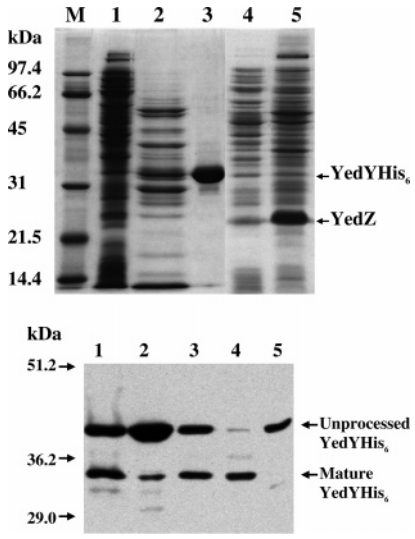

FIGURE 2: SDS−PAGE and Western immunoblot analysis of $YedYHis_6$ and YedZ. (a) SDS polyacrylamide gel of YedYZ amplification and purification. A composite of two gels is shown. Lane 1, SJB20-pMSYZ3 whole cells; lane 2, periplasm fraction; lane 3, purified $YedYHis_6$; lane 4, French press extract; lane 5, cytoplasmic membrane fraction. Positions of molecular weight markers, YedZ, and processed $YedYHis_6$ are indicated. (b) Western immunoblot of $YedYHis_6$ in whole cells and cell fractions of *E. coli* strains containing pMSYZ3 plasmid. Lanes 1−4: TG1 cells. Lane 1, whole cells; lane 2, 8000*g* pellet after French Press lysis of cells (indicates inclusion bodies); lane 3, cytoplasmic membrane preparation; lane 4, 150 000*g* supernatant. Lane 5, DSS640 (TG1 Δ*tatABCD*) whole cells. Positions of uncleaved and processed $YedYHis_6$ are indicated.

inducible pMS119 vector, was used for expression-testing in a number of common laboratory strains. *E.* coli HB101 had the highest expression levels of YedY and YedZ; however, a large amount of YedY formed inclusion bodies, even though YedZ appeared properly folded and inserted in the membrane (results not shown). *E. coli* TG1 showed slightly lower overall YedY expression, but a higher yield of mature processed YedY (Figure 2) with fewer inclusion bodies. The $YedYHis_6$ protein in inclusion bodies is almost exclusively unprocessed, as observed by Western immunoblot (Figure 2). Therefore, HB101 was used for studies of amplified YedZ in cytoplasmic membrane vesicles, while YedY was purified from a derivative of TG1 (see following text). Regardless of strain, we noted that YedY was found predominantly in the periplasm and did not exist as a stable membrane-associated complex with YedZ in equimolar amounts.

Purification of $YedYHis_6$. In an attempt to increase the yield of mature active $YedYHis_6$, we examined expression of $YedYHis_6$ in *E. coli* SJB20/pMSYZ3, a *mobA* derivative of TG1. The SJB20 strain produces the MPT form of the molybdenum cofactor but not the MGD form (*38*). Better expression in *mobA* strains has been observed with the cloned molybdenum domains from human sulfite oxidase (*39*) and spinach nitrate reductase (*40*) presumably due to the higher concentration of MPT in a *mobA* strain versus a wild-type strain. $YedYHis_6$ was amplified in *E. coli* SJB20 and purified from the periplasm by nickel affinity chromatography (Figure 2), as described in Experimental Procedures. Approximately 20 mg purified mature $YedYHis_6$ was obtained from ∼30 g of cell paste.

Physiological Role of YedYZ. We used several methods to search for a potential substrate or physiological role of YedYZ. An *E. coli yedYZ* deletion strain, SJB12, was constructed by the λ_{red} recombinase method (*17*). The phenotypes of SJB12 and its parent strain, MC4100, were identical in all studies, including growth in minimal media with various carbon, nitrogen, sulfur, or phosphorus sources, done by Biolog phenotype microtiter array (*41*), anaerobic growth using various terminal electron acceptors such as DMSO, trimethylamine-*N*-oxide (TMAO), and nitrate, and susceptibility to growth inhibitors such as heavy metals or oxidizing agents. We also attempted to identify a potential substrate for YedY(Z) by screening *E. coli* crude extracts containing overexpressed YedYZ in oxidoreductase assays, including established assays for sulfite oxidase (*42*), nitrate reductase (*23*, *24*), aldehyde dehydrogenase (*43*), and a variety of other substrates and artificial electron acceptors or donors. These assays were not successful (results not shown). However, when purified $YedYHis_6$ was subjected to the same screening procedures, the enzyme was able to catalyze the reduction of DMSO and TMAO using reduced benzyl viologen (BV) as an electron donor (*12*, *23*, *24*). $YedYHis_6$ was also able to catalyze the reduction of phenylmethyl sulfoxide, methionine sulfoxide, and tetramethylene sulfoxide (tetrahydrothiophene 1-oxide). However, $YedYHis_6$ showed no significant activity for various pyridine *N*-oxides, adenosine *N*-oxide, chlorate, or hydroxylamine as substrates.

$YedYH_6$ Spectroscopic Analysis. As prepared, purified $YedYHis_6$ has a slightly pink color. Its optical absorbance spectrum shows a peak centered at approximately 360 nm and a broad peak centered at 503 nm (Figure 3). The pink color was abolished upon addition of an excess amount of sodium dithionite (∼2 mM), and this is reflected by the loss of the 503 nm absorption band, and likely bleaching of the peak at 360 nm as well, although the spectrum is complicated by the strong absorbance of dithionite in this region. It is notable that EPR spectra reveal that the as-prepared spectrum of $YedYHis_6$ in Figure 3 corresponds to the spectrum of the protein exclusively containing the Mo(V) redox state of the Mo-MPT (see following text).

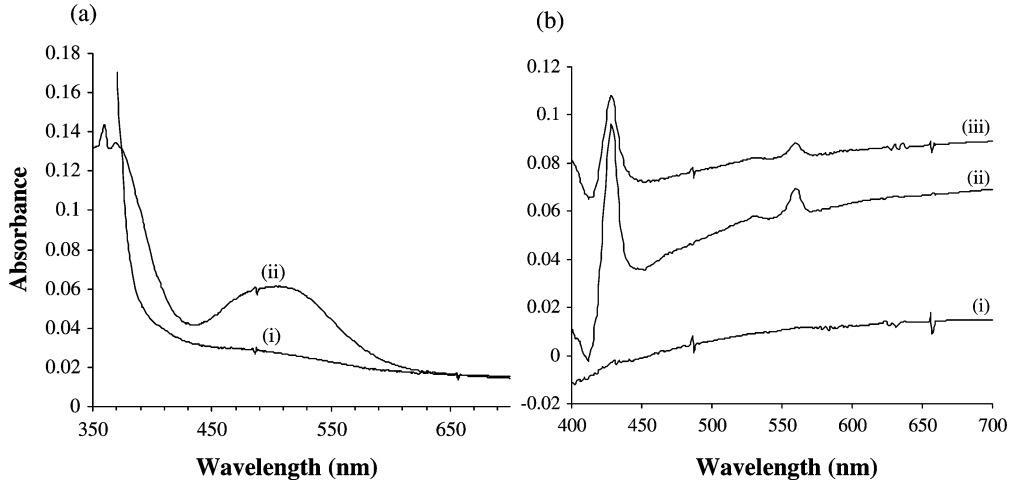

FIGURE 3: Visible absorption spectra of YedY and YedZ. (a) Spectra of 0.5 mg/mL (~15 μM) YedYHis$_6$ after reduction with 2 mM sodium dithionite (i) or as-purified (ii). (b) Spectra of cytoplasmic membrane preparations at a protein concentration of 1.0 mg/mL. (i), dithionite reduced minus air-oxidized spectrum of HB101-pMS119 (negative control) membranes; (ii), dithionite reduced minus oxidized spectrum of HB101-pMSYZ3 (YedZ-amplified) membranes; (iii), spectrum of HB101-pMSYZ3 membranes reduced anaerobically with 0.5 mM menadiol minus oxidized membranes. In panel b, the spectrum lines have been offset by arbitrary values to aid in presentation.

The molybdenum cofactor within purified YedYHis$_6$ was examined by EPR. Figure 4 shows the EPR spectrum of the as-isolated YedYHis$_6$ recorded at 50 K. Essentially similar spectra were recorded at 150 K (data not shown). The spectral features can be interpreted as arising from an axial Mo(V) species with $g_1 = 2.031$ and $g_{2,3} = 1.976$. In the low-field region of the spectrum, a hyperfine splitting of the g_1 feature is due to the interaction between the unpaired electron of the Mo(V) and the nuclear spin ($I = 5/2$) of the ^{95}Mo and ^{97}Mo isotopes with a hyperfine splitting constant of approximately 54 G. The hyperfine splitting of the other two *g*-tensors is too complex to be resolved directly from the spectra presented in Figure 4. Curiously, the EPR spectral features of the as-isolated YedYHis$_6$ did not diminish following incubation with excess potassium ferricyanide, indicating the E_m of the Mo(V) → Mo(VI) transition is unusually high. To further investigate this issue, we analyzed the EPR properties of YedYHis$_6$ by potentiometric analysis. Figure 4 shows a representative plot of the $g_{2,3}$ signal intensity versus E_h with samples being taken from a titration carried out in the oxidizing direction. Inspection of the data reveals that oxidation of the Mo(V) species to Mo(VI) was not possible, even when samples were potentiometrically poised at potentials greater than 350 mV for extended periods. Oxidative and reductive redox titrations result in midpoint potential ($E_{m,7}$) estimates of 130 ± 9 mV ($n = 1.3 \pm 0.09$; three determinations) and 134 ± 6 mV ($n = 1.63 \pm 0.05$; four determinations), respectively. The consistent observation of an *n*-value greater than 1.0 is consistent with the Mo(IV) → Mo(V) transition being weakly coupled to a 2-electron redox transition occurring in close proximity to the Mo atom. Possible candidates for this transition include redox interconversions of the pyranopterin (*44*, *45*), a redox interconversion of a tightly bound substrate, or an interconversion of an amino acid side chain.

In an attempt to shed further light on the behavior of the Mo-MPT cofactor, we performed redox titrations at pH 6 (in MES buffer) and at pH 8 (in Tricine buffer), resulting in estimates of the E_m of the Mo(IV) → Mo(V) transition of 145 and 128 mV, respectively. In neither case was a Mo(V) → Mo(VI) transition observed. Also, no evidence for a tightly coupled proton was observed at pH 6.

Tungsten-Substituted YedYHis$_6$. YedYHis$_6$ was also amplified and purified from cells of *E. coli* SJB20/pMSYZ3 grown in the presence of 10 mM Na_2WO_4 rather than 1 mM Na_2MoO_4. The yield of soluble tungsten-substituted YedYHis$_6$, approximately 5 mg from 30 g of cell paste, was lower than that of the molybdenum form. The preparation was colorless and had no observable absorption bands in the 350−700 nm range (result not shown). The protein was inactive with benzyl viologen as an electron donor, using *S*- or *N*-oxides as substrates. No activity was observed in an "oxidase" assay using trimethylamine or methionine as electron donors and oxidized dichlorophenolindolphenol as an electron acceptor dye, as has been used for assay of dimethyl sulfide dehydrogenase (*46*).

No W(V) EPR signal was observed in the as-isolated tungsten-substituted form of the enzyme. However, the recently determined crystal structure of tungsto-YedY (*12*) is essentially identical to that of the molybdo form, including the presence of the W-MPT cofactor.

Analysis of YedZ. Cytoplasmic membrane vesicles containing amplified YedZ were prepared from *E. coli* HB101/pMSYZ3 as described in the Experimental Procedures. The membranes were dark red, indicating the presence of heme. The visible absorbance spectrum of dithionite-reduced *minus* oxidized membrane spectra showed a Soret band at 428 nm, an α-band at 559 nm, and a β-band at 530 nm (Figure 3). These features are characteristic for the presence of a *b*-type heme in YedZ. Under anaerobic conditions, the YedZ heme was also reduced by menadiol, a menaquinol analogue, as well as by other menaquinol and ubiquinol analogues (not shown). Thus, in vivo YedZ may interact with the quinol pool in the cytoplasmic membrane and play a role in shuttling electrons to or from other membrane-associated oxidoreductases.

Cytoplasmic membrane vesicles containing amplified YedZ were also analyzed by EPR (Figure 5). The heme of YedZ has an EPR spectrum with a single peak corresponding to the g_z of a HALS (*h*ighly *a*nisotropic *l*ow *s*pin) heme with

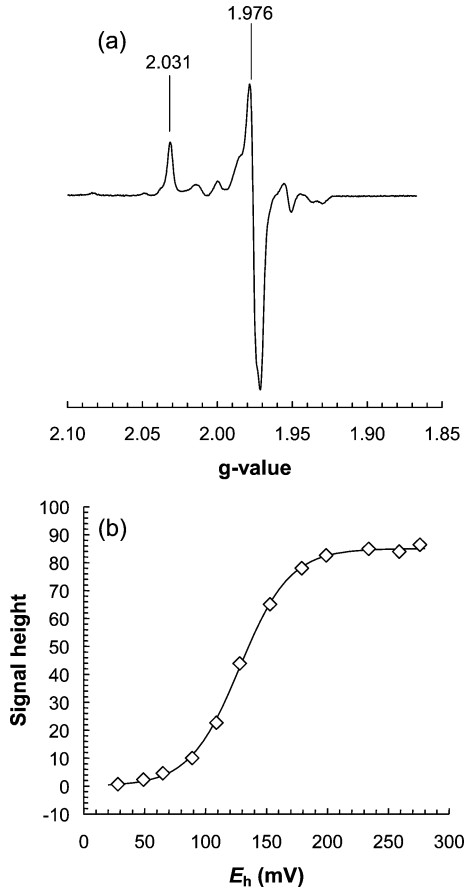

FIGURE 4: EPR characterization of the Mo-MPT of YedY−His_6. (a) Mo(V) EPR spectrum of as-isolated YedY. The spectrum was recorded at 50 K using 2 mW microwave power at 9.382 GHz and a modulation amplitude of 4 G_{pp}. The sample contains 2.2 mg/mL purified YedYHis_6. (b) Redox titration of the YedYHis_6 Mo(V) EPR spectrum. Shown is a representative redox titration in the oxidizing of the intensity of the $g_{2,3}$ peak-trough of the YedY Mo(V) EPR spectrum (the $g = 1.976$ peak-trough). Data were fit to a single $n = 1.25$ species with an E_m value of +128 mV. Samples were redox-poised for at least 5 min at 25 °C at pH 7 in 100 mM MOPS and 5 mM EDTA prior to rapid freezing in liquid nitrogen-chilled ethanol. EPR spectra were recorded at 150 K.

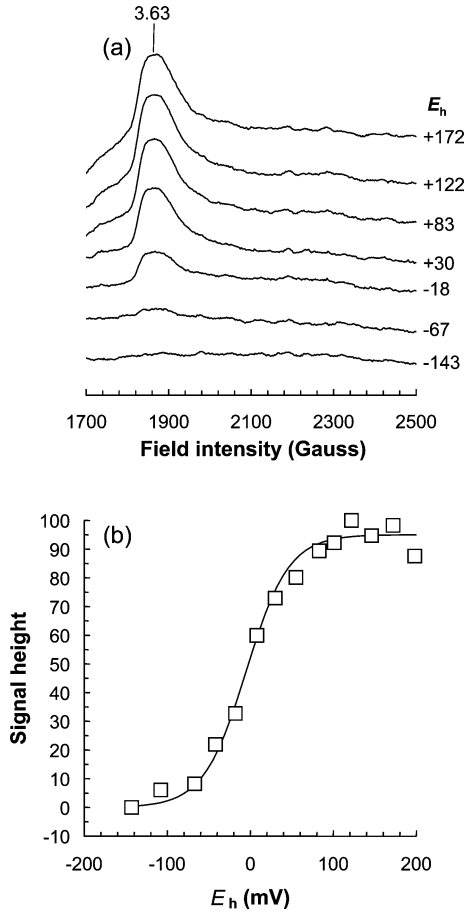

FIGURE 5: Potentiometric titration of HB101 membrane enriched in YedZ. EPR spectrum of YedZ in cytoplasmic membrane vesicles. (a) EPR spectra of potentiometrically poised samples at the potential (E_h) indicated in mV. Spectra were recorded under the following conditions: temperature, 12 K; microwave power, 100 mW at 9.47 GHz; modulation amplitude, 10 G_{pp} at 100 kHz. In each case, three scans were accumulated. The potentiometric titration was carried out at approximately 30 mg/mL protein at pH 7.0 in 100 mM MOPS and 5 mM EDTA. (b) Plot of the intensity of the $g = 3.63$ peak versus E_h. The peak intensity was derived from a three-point drop line analysis of spectra such as those in panel a. The solid line represents an $n = 1$ fit to the Nernst equation with an $E_{m,7}$ of −5 mV.

bishistidine protein coordination (*47*). As expected for this type of heme, the other two *g*-tensors (g_x and g_y) were not observed (*48*). Figure 5a shows spectra of redox-poised membranes recorded at 12 K, and Figure 5b shows a plot of the intensity of the $g = 3.63$ feature versus E_h. The heme of YedZ titrates as an $n = 1.0$ species with an $E_{m,7}$ of -8 ± 16 mV (three determinations). Careful EPR examination of the membrane preparations at 50 K did indicate a signal attributable to the molybdenum of YedY (data not shown); however, this signal was of very low intensity. Similarly, we found very little YedY on the membrane as determined by SDS−polyacrylamide gel electrophoresis and Western immunoblotting of SJB20-pMSYZ3 membrane preparations (Figure 2).

Cys102Ser YedY and Interaction with YedZ. The active site Cys102 of YedY was changed to serine, and the properties of the resulting protein were examined. As shown by the Western immunoblot in Figure 6, Cys102Ser YedY remained almost exclusively in the cytoplasmic membrane fraction, unlike wild-type YedY which was found in the periplasm. To determine whether the membrane association

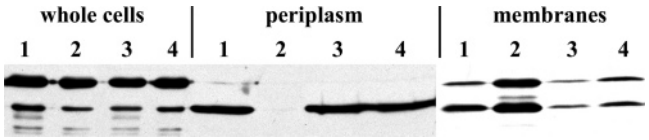

FIGURE 6: Subcellular localization of wild-type and Cys102Ser YedYHis_6. Anti-His tag Western immunoblot shows unprocessed and mature forms of YedYHis_6 (top and bottom major bands, respectively). SJB20 cells were used and samples prepared as indicated in the Experimental Procedures. Samples: 1, pMSYZ4(WT), containing wild-type YedYHis_6 and YedZ; 2, pMSYZ4(C102S) containing Cys102Ser YedYHis_6 and YedZ; 3, pMSYH6(WT) containing wild-type YedYHis_6 alone; 4, pMSYH6(C102S) containing Cys102Ser YedYHis_6 alone.

of C102S YedY required the presence of YedZ, C102S YedY was amplified from the plasmid pMSYH6, which did not contain the *yedZ* gene. In this case, the C102S YedY remained soluble in the periplasm (Figure 6), indicating that indeed C102S YedY associates specifically with YedZ in the cytoplasmic membrane. Purified C102S YedY has no detectable enzyme activity but appears to assemble the MPT

cofactor, as indicated by assay of the fluorescent "Form A" derivative of the cofactor (*49*) (results not shown).

DISCUSSION

We report the cloning, amplification, and purification of a molybdenum-containing sulfite oxidase homologue from *E. coli*, YedYZ. YedY was identified as the soluble periplasmic catalytic subunit of the oxidoreductase and contains a molybdo-molybdopterin form of the molybdenum cofactor.

Purified YedYHis$_6$ presents some novel spectroscopic features. EPR experiments reveal that the Mo(VI) redox state appears to be inaccessible, even following incubation at high E_h-values. One consequence of this is that the optical spectrum of Figure 3a corresponds to the Mo(V) form of the enzyme (absorption bands at approximately 360 and 503 nm). Optical spectra of sulfite oxidase are often complicated by the presence of its heme-binding domain. However, the Mo-MPT binding domain of human sulfite oxidase can be prepared by heterologous expression. Its oxidized spectrum exhibits absorption bands at approximately 360 and 480 nm (*50*). The oxidized spectrum of the Mo-MPT binding domain of rat liver sulfite oxidase has an almost identical spectrum (*51*). The plant sulfite oxidase from *A. thaliana* lacks the heme domain and also has absorption bands at approximately 360 and 480 nm. Thus, the appearance of an absorption band at 503 nm in purified YedYHis$_6$ may be a result of the Mo(V) redox state of its cofactor (*52*).

Interpretation of the coordination sphere of the molybdenum of Mo-MPT-containing enzymes on the basis of EPR data alone is not straightforward. However, the recent availability of several protein structures has made qualitative comparisons insightful. The $g_{1,2,3}$-values of the Mo(V) species of YedYHis$_6$ are approximately 2.031, 1.976, and 1.976, respectively, with a g_{av} of 1.994. Also, there is no evidence in our data suggesting the presence of coupled proton at low-pH values. Of the Mo(V) EPR spectra published for a range of enzyme systems, that of YedYHis$_6$ most closely resembles that of the hydroxymethylpurine adduct to xanthine dehydrogenase (*53*, *54*) (corresponding to the "very rapid" reaction intermediate). This has Mo(V) coordinated by the two dithiolene sulfurs (from the pyranopterin), an oxo group, a sulfido group, and an oxygen from the substrate. The structure of YedY (*12*) reveals that the most likely coordination sphere of the Mo(V) involves two dithiolene sulfurs, a sulfur from the protein-Mo ligand (C102), and two oxygens.

Given the structural similarity between YedYHis$_6$ and sulfite oxidase (*12*), some similarity would also be expected between the EPR properties of the two enzymes. The Mo(V) spectrum of YedYHis$_6$ is somewhat similar to that of the low-pH form of sulfite oxidase recorded in D_2O in which the proton hyperfine coupling has been eliminated ($g_{1,2,3}$ values of 2.007, 1.974, 1.968; g_{av} = 1.983) (*55*). A number of model compounds have been synthesized to mimic molybdoenzyme Mo coordination environments, some of which have EPR spectra similar to that of YedYHis$_6$. One of these, a six-coordinate compound containing a dithiolate coordinated to a [**L**-Mo(V)O]$^{2+}$ unit (**L** = hydrotris(3,5-dimethyl-1-pyrazolyl)borate), has a similar EPR spectrum to that of YedYHis$_6$ with $g_{1,2,3}$ values of 2.022, 1.960, and 1.932 (g_{av} = 1.971) (*55*). This compound coordinates the Mo(V) via three nitrogen atoms, one oxo oxygen, and two sulfur atoms. However, this coordination environment is at odds with that observed for YedYHis$_6$ which comprises two dithiolene sulfurs, an oxo group, and a sulfur from Cys102, with an additional oxygen ligand being provided by an unidentified moiety located at the bottom of the substrate binding funnel (*12*). Another oxomolybdenum complex, [MoO(V)(SPh)$_4$]$^-$, has an EPR spectrum with $g_{1,2,3}$ values of 2.017, 1.979, and 1.979 (g_{av} = 1.990) (*56*). In this case, coordination is provided by four sulfurs and one oxo group. Thus, neither of the model compounds discussed above provide Mo coordination that is completely consistent with the structure of YedYHis$_6$ determined by X-ray crystallography. A complete understanding of the Mo(V) coordination environment of YedYHis$_6$ will thus require identification of the electron density observed in the substate binding site by Loschi et al. (*12*). We are currently using a combination of X-ray crystallography and spectroscopy to pursue this objective.

The Mo-MPT cofactor of YedY exhibits unusual potentiometric behavior. In most molybdenum enzymes, the IV, V, and VI redox states are readily accessible. In YedY, only the IV and V states are attainable under the conditions reported herein. In this respect, it is similar to a site-directed mutant of the protein-Mo ligand of the membrane-bound DMSO reductase of *E. coli* (DmsABC). In this mutant (DmsA-Ser205Ala), the Mo(VI) state also appears to be unattainable in potentiometric titrations (*57*). In the case of YedY, the apparent inability to achieve the Mo(VI) redox state has implications for the catalytic mechanism of the enzyme. Specifically, if the Mo is the only redox active component present, it is likely that two-electron substrate reduction/oxidation would have to be carried out in discreet one-electron steps. Further complications arise if YedY is indeed soluble and has to dock with YedZ to pick up or donate electrons singly. Overall, the apparent one-electron capacity of YedY may explain the relatively low turnover number calculated for its reduction of DMSO and TMAO substrates, approximately 5 and 19 s^{-1}, respectively (*12*). Intriguingly, we have obtained some evidence that YedY increases its apparent electron availability by coupling its Mo(IV) → Mo(V) transition with an $n > 1$ redox transition, possibly involving redox chemistry of the pyranopterin (*44*, *45*).

EPR spectroscopy reveals that YedZ contains a HALS-type low-spin heme with an $E_{m,7}$ value of −8 mV. This suggests a thermodynamically "downhill" transfer of electrons to the Mo-MPT of YedY, consistent with YedYZ comprising a quinol oxidizing and reductase system in *E. coli*. HALS-type EPR spectra are commonly associated with hydrophobic cytochromes *b*, which play a role in quinol oxidation, the most prominent example being that of the hemes of the cytochrome *b* subunit of mitochondrial complex III (*58*, *59*). Little structural information is available for YedZ beyond its predicted topology and orientation within the cytoplasmic membrane (Figure 1). Future studies will focus on identifying its quinol-binding site, its quinol preference (menaquinol versus ubiquinol), and characterization of its heme iron coordination by site-directed mutagenesis.

The X-ray crystal structure of YedYHis$_6$ (*12*) shows that, despite weak sequence similarity, it has a fold similar to the structures of the Mo-MPT-containing domains of sulfite oxidases from chicken and *A. thaliana*, with root-mean-

square deviations of 1.7 and 2.2 Å, respectively. The active site of YedY bears some similarity to the sulfite oxidases, notably with the involvement of a molybdenum-coordinating Cys residue (Cys102). However, other residues in the active site are much different, which might explain the differences in kinetic parameters between YedY and other sulfite oxidase family members. Data in this report, as well as the crystal structure, indicate that YedY and its many orthologs represent a new but well-represented branch of the sulfite oxidase family of molybdoenzyme, a family previously thought to be almost exclusively found in eukaryotes.

We have found that YedY is able to catalyze the reduction of *S*- and *N*-oxides but were unable to demonstrate oxidation of substrates such as sulfite and TMA. To our knowledge, no members of the sulfite oxidase family have been shown to catalyze *S*- and *N*-oxide reduction. Other *S*- and *N*-oxide reductases exist in *E. coli*, namely, DmsABC (*23*, *60*), YnfEFGH (*61*), TorCAD (*62*), and TorYZ (*63*), and these enzymes have been well-characterized. It appears that YedYZ does not function as a respiratory *S*- and *N*-oxide reductase as *dmsABC* and *dmsABC*/*torA* gene knockouts fail to grow anaerobically with DMSO or TMAO as terminal electron acceptors, respectively (*24*, *64*). Complementation of the *dmsABC* knockout strain with pMSYZ3 did not allow for growth (results not shown). This is again in agreement with the kinetic data (*12*), in that YedY is able to catalyze these reactions with much lower k_{cat} than the Dms or Tor systems.

The tungsten-substituted form of YedY was also prepared in this study, and the crystal structure of the protein has been determined (*12*). The structures of the tungsten and molybdenum forms of YedY are virtually identical, including the MPT cofactor. However, the tungsten-substituted YedY was inactive in enzyme assays. This is in contrast to the MobisMGD-containing enzymes DorA DMSO reductase from *Rhodobacter capsulatus* (*65*) and TorA TMAO reductase from *E. coli* (*66*), both of which retain activity in the tungsten-substituted form, although with altered kinetic properties. However, the tungsten-substituted sulfite oxidase from rat liver retains its MPT cofactor but is inactive (*67*).

Well-known *E. coli* molybdenum-containing oxidoreductases with integral membrane subunits, such as NarGHI nitrate reductase and DmsABC DMSO reductase, form stable membrane-bound complexes. YedYZ differs from these enzymes; the results presented herein show that processed wild-type YedYHis$_6$ did not associate with YedZ in appreciable amounts but instead remained in the periplasm. This finding led us to doubt whether YedY and YedZ actually formed a complex at all. However, mutation of the YedY active site residue Cys102 to Ser resulted in a dramatically different location of the YedY subunit; processed Cys102Ser YedYHis$_6$ targeted very efficiently to the cytoplasmic membrane, and specifically to YedZ (Figure 6). The reason for such a dramatic change in subcellular localization remains unclear. The change cannot simply be due to an absence of catalytic turnover in the C102S mutant, as the tungsten-substituted YedYHis$_6$, which is also inactive, was purified from the periplasm. There may be direct structural changes associated with the Cys102Ser mutation, although C102S YedY still retains its Mo-MPT cofactor. Nevertheless, a specific interaction between YedY and YedZ has been demonstrated, and the two subunits are likely coupled during catalysis in vivo.

The optimal substrate or precise physiological role for YedYZ in *E. coli* and its well-conserved orthologs in other bacteria remains unknown. The existence within the *E. coli* and other genomes of genes encoding such highly conserved enzyme systems of unknown function is likely to reflect a previously unforseen metabolic diversity. Careful scrutiny of such diversity may reveal the existence of unanticipated and potentially biotechnologically relevant interconversions within the *E. coli* metabolome.

ACKNOWLEDGMENT

We thank Dr. Tracy Palmer, University of East Anglia, U.K., for the TP1000 strain. The technical assistance of Gillian Shaw, Delilah Mroczko, and Janice Chen is greatly appreciated. We also thank the laboratory of Dr. Chris Le, Department of Public Health Sciences, University of Alberta, Canada, for performing mass spectrometry experiments in support of this work.

REFERENCES

1. Cole, S. T. (1982) Nucleotide sequence coding for the flavoprotein subunit of the fumarate reductase of *Escherichia coli*, *Eur. J. Biochem. 122*, 479−484.
2. Cole, S. T., Grundstrom, T., Jaurin, B., Robinson, J. J. and Weiner, J. H. (1982) Location and nucleotide sequence of frdB, the gene coding for the iron-sulphur protein subunit of the fumarate reductase of *Escherichia coli*, *Eur. J. Biochem. 126*, 211−216.
3. Wood, D., Darlison, M. G., Wilde, R. J., and Guest, J. R. (1984) Nucleotide sequence encoding the flavoprotein and hydrophobic subunits of the succinate dehydrogenase of *Escherichia coli*, *Biochem. J. 222*, 519−534.
4. Blasco, F., Iobbi, C., Giordano, G., Chippaux, M., and Bonnefoy, V. (1989) Nitrate reductase of *Escherichia coli*: completion of the nucleotide sequence of the nar operon and reassessment of the role of the alpha and beta subunits in iron binding and electron transfer, *Mol. Gen. Genet. 218*, 249−256.
5. Bilous, P. T., Cole, S. T., Anderson, W. F., and Weiner, J. H. (1988) Nucleotide sequence of the dmsABC operon encoding the anaerobic dimethylsulphoxide reductase of *Escherichia coli*, *Mol. Microbiol. 2*, 785−795.
6. Johnson, J. L., Hainline, B. E., and Rajagopalan, K. V. (1980) Characterization of the molybdenum cofactor of sulfite oxidase, xanthine, oxidase, and nitrate reductase. Identification of a pteridine as a structural component, *J. Biol. Chem. 255*, 1783−1786.
7. Hille, R. (1996) The mononuclear molybdenum enzymes, *Chem. Rev. 96*, 2757−2816.
8. Moura, J. J., Brondino, C. D., Trincao, J., and Romao, M. J. (2004) Mo and W bis-MGD enzymes: nitrate reductases and formate dehydrogenases, *J. Biol. Inorg. Chem. 9*, 791−799.
9. Hille, R. (2002) Molybdenum and tungsten in biology, *Trends Biochem. Sci. 27*, 360−367.
10. Kisker, C., Schindelin, H., and Rees, D. C. (1997) Molybdenum-cofactor-containing enzymes: structure and mechanism, *Annu. Rev. Biochem. 66*, 233−267.
11. Blattner, F. R., Plunkett, G., III, Bloch, C. A., Perna, N. T., Burland, V., Riley, M., Collado-Vides, J., Glasner, J. D., Rode, C. K., Mayhew, G. F., Gregor, J., Davis, N. W., Kirkpatrick, H. A., Goeden, M. A., Rose, D. J., Mau, B., and Shao, Y. (1997) The complete genome sequence of *Escherichia coli* K-12, *Science 277*, 1453−1474.
12. Loschi, L., Brokx, S. J., Hills, T. L., Zhang, G., Bertero, M. G., Lovering, A. L., Weiner, J. H., and Strynadka, N. C. (2004) Structural and biochemical identification of a novel bacterial oxidoreductase, *J. Biol. Chem. 279*, 50991−50400.
13. Sambrook, J., and Russell, D. W. (2001) *Molecular Cloning*: *A Laboratory Manual*, 3rd ed., Cold Spring Harbor Laboratory Press, Cold Spring Harbor, NY.
14. Markwell, M. A., Haas, S. M., Bieber, L. L., and Tolbert, N. E. (1978) A modification of the Lowry procedure to simplify protein determination in membrane and lipoprotein samples, *Anal. Biochem. 87*, 206−210.

15. Strack, B., Lessl, M., Calendar, R., and Lanka, E. (1992) A common sequence motif, -E−G-Y-A-T-A-, identified within the primase domains of plasmid-encoded I- and P-type DNA primases and the alpha protein of the *Escherichia coli* satellite phage P4, *J. Biol. Chem. 267*, 13062−13072.
16. Sambasivarao, D., Dawson, H. A., Zhang, G., Shaw, G., Hu, J., and Weiner, J. H. (2001) Investigation of *Escherichia coli* dimethyl sulfoxide reductase assembly and processing in strains defective for the sec-independent protein translocation system membrane targeting and translocation, *J. Biol. Chem. 276*, 20167−20174.
17. Datsenko, K. A., and Wanner, B. L. (2000) One-step inactivation of chromosomal genes in *Escherichia coli* K-12 using PCR products, *Proc. Natl. Acad. Sci. U.S.A. 97*, 6640−6645.
18. Millller, J. H. (1992) *A Short Course in Bacterial Genetics. A Laboratory Manual and Handbook for Escherichia coli and Related Bacteria*, Cold Spring Harbor Laboratory Press, Cold Spring Harbor, NY.
19. Bilous, P. T., and Weiner, J. H. (1985) Dimethyl sulfoxide reductase activity by anaerobically grown *Escherichia coli* HB101, *J. Bacteriol. 162*, 1151−1155.
20. Johnson, J. L., Indermaur, L. W., and Rajagopalan, K. V. (1991) Molybdenum cofactor biosynthesis in *Escherichia coli*. Requirement of the chlB gene product for the formation of molybdopterin guanine dinucleotide, *J. Biol. Chem. 266*, 12140−12145.
21. Rothery, R. A., and Weiner, J. H. (1991) Alteration of the iron−sulfur cluster composition of *Escherichia coli* dimethyl sulfoxide reductase by site-directed mutagenesis, *Biochemistry 30*, 8296−8305.
22. Rothery, R. A., Trieber, C. A., and Weiner, J. H. (1999) Interactions between the molybdenum cofactor and iron−sulfur clusters of *Escherichia coli* dimethylsulfoxide reductase, *J. Biol. Chem. 274*, 13002−13009.
23. Simala-Grant, J. L., and Weiner, J. H. (1996) Kinetic analysis and substrate specificity of *Escherichia coli* dimethyl sulfoxide reductase, *Microbiology 142* (Pt 11), 3231−3239.
24. Sambasivarao, D., and Weiner, J. H. (1991) Dimethyl sulfoxide reductase of *Escherichia coli*: an investigation of function and assembly by use of in vivo complementation, *J. Bacteriol. 173*, 5935−5943.
25. Sargent, F., Bogsch, E. G., Stanley, N. R., Wexler, M., Robinson, C., Berks, B. C., and Palmer, T. (1998) Overlapping functions of components of a bacterial Sec-independent protein export pathway, *EMBO J. 17*, 3640−3650.
26. Weiner, J. H., Bilous, P. T., Shaw, G. M., Lubitz, S. P., Frost, L., Thomas, G. H., Cole, J. A., and Turner, R. J. (1998) A novel and ubiquitous system for membrane targeting and secretion of cofactor-containing proteins, *Cell 93*, 93−101.
27. Stanley, N. R., Palmer, T., and Berks, B. C. (2000) The twin arginine consensus motif of Tat signal peptides is involved in Sec-independent protein targeting in *Escherichia coli*, *J. Biol. Chem. 275*, 11591−11596.
28. Mori, H., Isono, K., Horiuchi, T., and Miki, T. (2000) Functional genomics of *Escherichia coli* in Japan, *Res. Microbiol. 151*, 121−128.
29. Perna, N. T., Plunkett, G., III, Burland, V., Mau, B., Glasner, J. D., Rose, D. J., Mayhew, G. F., Evans, P. S., Gregor, J., Kirkpatrick, H. A., Posfai, G., Hackett, J., Klink, S., Boutin, A., Shao, Y., Miller, L., Grotbeck, E. J., Davis, N. W., Lim, A., Dimalanta, E. T., Potamousis, K. D., Apodaca, J., Anantharaman, T. S., Lin, J., Yen, G., Schwartz, D. C., Welch, R. A., and Blattner, F. R. (2001) Genome sequence of enterohaemorrhagic *Escherichia coli* O157:H7, *Nature*. *409*, 529−533.
30. Hayashi, T., Makino, K., Ohnishi, M., Kurokawa, K., Ishii, K., Yokoyama, K., Han, C. G., Ohtsubo, E., Nakayama, K., Murata, T., Tanaka, M., Tobe, T., Iida, T., Takami, H., Honda, T., Sasakawa, C., Ogasawara, N., Yasunaga, T., Kuhara, S., Shiba, T., Hattori, M., and Shinagawa, H. (2001) Complete genome sequence of enterohemorrhagic *Escherichia coli* O157:H7 and genomic comparison with a laboratory strain K-12, *DNA Res. 8*, 11−22.
31. Welch, R. A., Burland, V., Plunkett, G., III, Redford, P., Roesch, P., Rasko, D., Buckles, E. L., Liou, S. R., Boutin, A., Hackett, J., Stroud, D., Mayhew, G. F., Rose, D. J., Zhou, S., Schwartz, D. C., Perna, N. T., Mobley, H. L., Donnenberg, M. S., and Blattner, F. R. (2002) Extensive mosaic structure revealed by the complete genome sequence of uropathogenic *Escherichia coli*, *Proc. Natl. Acad. Sci. U.S.A. 99*, 17020−17024.
32. Altschul, S. F., Madden, T. L., Schaffer, A. A., Zhang, J., Zhang, Z., Miller, W., and Lipman, D. J. (1997) Gapped BLAST and PSI-BLAST: a new generation of protein database search programs, *Nucleic Acids Res. 25*, 3389−3402.
33. Kappler, U., Bennett, B., Rethmeier, J., Schwarz, G., Deutzmann, R., McEwan, A. G., and Dahl, C. (2000) Sulfite:cytochrome *c* oxidoreductase from *Thiobacillus novellus*. Purification, characterization, and molecular biology of a heterodimeric member of the sulfite oxidase family, *J. Biol. Chem. 275*, 13202−13212.
34. Neame, P. J., and Barber, M. J. (1989) Conserved domains in molybdenum hydroxylases. The amino acid sequence of chicken hepatic sulfite oxidase, *J. Biol. Chem. 264*, 20894−20901.
35. Prosser, I. M., and Lazarus, C. M. (1990) Nucleotide sequence of a spinach nitrate reductase cDNA, *Plant Mol. Biol. 15*, 187−190.
36. Schrader, N., Fischer, K., Theis, K., Mendel, R. R., Schwarz, G., and Kisker, C. (2003) The crystal structure of plant sulfite oxidase provides insights into sulfite oxidation in plants and animals, *Structure 11*, 1251−1263.
37. Drew, D., Sjostrand, D., Nilsson, J., Urbig, T., Chin, C. N., de Gier, J. W., and von Heijne, G. (2002) Rapid topology mapping of *Escherichia coli* inner-membrane proteins by prediction and PhoA/GFP fusion analysis, *Proc. Natl. Acad. Sci. U.S.A. 99*, 2690−2695.
38. Palmer, T., Santini, C. L., Iobbi-Nivol, C., Eaves, D. J., Boxer, D. H., and Giordano, G. (1996) Involvement of the narJ and mob gene products in distinct steps in the biosynthesis of the molybdoenzyme nitrate reductase in *Escherichia coli*, *Mol. Microbiol. 20*, 875−884.
39. Temple, C. A., Graf, T. N., and Rajagopalan, K. V. (2000) Optimization of expression of human sulfite oxidase and its molybdenum domain, *Arch. Biochem. Biophys. 383*, 281−287.
40. Pollock, V. V., Conover, R. C., Johnson, M. K., and Barber, M. J. (2002) Bacterial expression of the molybdenum domain of assimilatory nitrate reductase: production of both the functional molybdenum-containing domain and the nonfunctional tungsten analog, *Arch. Biochem. Biophys. 403*, 237−248.
41. Bochner, B. R., Gadzinski, P., and Panomitros, E. (2001) Phenotype microarrays for high-throughput phenotypic testing and assay of gene function, *Genome Res. 11*, 1246−1255.
42. Wilson, H. L., and Rajagopalan, K. V. (2004) The role of tyrosine 343 in substrate binding and catalysis by human sulfite oxidase, *J. Biol. Chem. 279*, 15105−15113.
43. Mukund, S., and Adams, M. W. (1993) Characterization of a novel tungsten-containing formaldehyde ferredoxin oxidoreductase from the hyperthermophilic archaeon, *Thermococcus litoralis*. A role for tungsten in peptide catabolism, *J. Biol. Chem. 268*, 13592−13600.
44. Enemark, J. H., and Garner, C. D. (1997) The coordination chemistry and function of the molybdenum centres of the oxomolybdoenzymes, *J. Biol. Inorg. Chem. 2*, 817−822.
45. Nieter Burgmayer, S. J., Pearsall, D. L., Blaney, S. M., Moore, E. M., and Sauk-Schubert, C. (2004) Redox reactions of the pyranopterin system of the molybdenum cofactor, *J. Biol. Inorg. Chem. 9*, 59−66.
46. McDevitt, C. A., Hugenholtz, P., Hanson, G. R., and McEwan, A. G. (2002) Molecular analysis of dimethyl sulphide dehydrogenase from *Rhodovulum sulfidophilum*: its place in the dimethyl sulphoxide reductase family of microbial molybdopterin-containing enzymes, *Mol. Microbiol. 44*, 1575−1587.
47. Walker, F. A., Huynh, B. H., Scheidt, W. R., and Osvath, S. R. (1986) Models of the cytochromes *b*. Effect of axial ligand plane orientation on the EPR and Mössbauer spectra of low spin ferrihemes, *J. Am. Chem. Soc. 108*, 5288−5296.
48. Salerno, J. C. (1984) Cytochrome electron spin resonance lineshapes, ligand fields, and components stoichiometry in ubiquinol-cytochrome *c* oxidoreductase, *J. Biol. Chem. 259*, 2331−2336.
49. Johnson, J. L., Hainline, B. E., Rajagopalan, K. V., and Arison, B. H. (1984) The pterin component of the molybdenum cofactor. Structural characterization of two fluorescent derivatives, *J. Biol. Chem. 259*, 5414−5422.
50. Garton, S. D., Garrett, R. M., Rajagopalan, K. V., and Johnson, M. K. (1997) Resonance Raman characterization of the molybdenum center in sulfite oxidase: identification of the Mo═O stretching modes, *J. Am. Chem. Soc. 119*, 2590−2591.
51. Garrett, R. M., and Rajagopalan, K. V. (1996) Site-directed mutagenesis of recombinant sulfite oxidase: identification of cysteine 207 as a ligand of molybdenum, *J. Biol. Chem. 271*, 7387−7391.
52. Eilers, T., Schwarz, G., Brinkmann, H., Witt, C., Richter, T., Nieder, J., Koch, B., Hille, R., Hansch, R., and Mendel, R. R. (2001) Identification and biochemical characterization of *Arabi-*

dopsis thaliana sulfite oxidase. A new player in plant sulfur metabolism, *J. Biol. Chem. 276*, 46989−46994.
53. Jones, R. M., Inscore, F. E., Hille, R., and Kirk, M. L. (1999) Freeze-quench magnetic circular dichroism spectroscopic study of the "very rapid" intermediate in xanthine oxidase, *Inorg. Chem. 38*, 4963−4970.
54. Choi, E. Y., Stockert, A. L., Leimkuhler, S., and Hille, R. (2004) Studies on the mechanism of action of xanthine oxidase, *J. Inorg. Biochem. 98*, 841−848.
55. Dhawan, I. K., and Enemark, J. H. (1996) EPR studies of oxomolybdenum(V) complexes with sulfur donor ligands: implications for the molybdenum center of sulfite oxidase, *Inorg. Chem. 35*, 4873−4882.
56. Hanson, G. R., Brunette, A. A., McDonell, A. C., Murray, K. S., and Wedd, A. G. (1981) Electronic properties of thiolate compounds of oxomolybdenum(V) and their tungsten and selenium analogues. Effects of ^{17}O, ^{98}Mo, and ^{95}Mo isotope substitution upon ESR spectra, *J. Am. Chem. Soc. 103*, 1953−1959.
57. Trieber, C. A., Rothery, R. A., and Weiner, J. H. (1996) Consequences of removal of a molybdenum ligand (DmsA-Ser-176) of *Escherichia coli* dimethyl sulfoxide reductase, *J. Biol. Chem. 271*, 27339−27345.
58. Saribas, A. S., Ding, H., Dutton, P. L., and Daldal, F. (1997) Substitutions at position 146 of cytochrome *b* affect drastically the properties of heme b_L and the Q_o site of *Rhodobacter capsulatus* cytochrome bc_1 complex, *Biochim. Biophys. Acta 1319*, 99−108.
59. Valkova-Valchanova, M. B., Saribas, A. S., Gibney, B. R., Dutton, P. L., and Daldal, F. (1998) Isolation and characterization of a two-subunit cytochrome bc_1 subcomplex from *Rhodobacter capsulatus* and reconstitution of its ubihydroquinone oxidation site (Q_o) site with purified Fe−S protein subunit, *Biochemistry 37*, 16242−16251.
60. Bilous, P. T., and Weiner, J. H. (1988) Molecular cloning and expression of the *Escherichia coli* dimethyl sulfoxide reductase operon, *J Bacteriol. 170*, 1511−1518.
61. Lubitz, S. P., and Weiner, J. H. (2003) The *Escherichia coli* ynfEFGHI operon encodes polypeptides which are paralogues of dimethyl sulfoxide reductase (DmsABC), *Arch. Biochem. Biophys. 418*, 205−216.
62. Mejean, V., Iobbi-Nivol, C., Lepelletier, M., Giordano, G., Chippaux, M., and Pascal, M. C. (1994) TMAO anaerobic respiration in *Escherichia coli*: involvement of the tor operon, *Mol. Microbiol. 11*, 1169−1179.
63. Gon, S., Patte, J. C., Mejean, V., and Iobbi-Nivol, C. (2000) The torYZ (yecK bisZ) operon encodes a third respiratory trimethylamine *N*-oxide reductase in *Escherichia coli*, *J. Bacteriol. 182*, 5779−5786.
64. Sambasivarao, D., and Weiner, J. H. (1991) Differentiation of the multiple S- and *N*-oxide-reducing activities of *Escherichia coli*, *Curr. Microbiol. 23*, 105−110.
65. Stewart, L. J., Bailey, S., Bennett, B., Charnock, J. M., Garner, C. D., and McAlpine, A. S. (2000) Dimethylsulfoxide reductase: an enzyme capable of catalysis with either molybdenum or tungsten at the active site, *J. Mol. Biol. 299*, 593−600.
66. Buc, J., Santini, C. L., Giordani, R., Czjzek, M., Wu, L. F., and Giordano, G. (1999) Enzymatic and physiological properties of the tungsten-substituted molybdenum TMAO reductase from *Escherichia coli*, *Mol. Microbiol. 32*, 159−168.
67. Johnson, J. L., and Rajagopalan, K. V. (1976) Electron paramagnetic resonance of the tungsten derivative of rat liver sulfite oxidase, *J. Biol. Chem. 251*, 5505−5511.

BI050621A